Stokes-Einstein violation in glass-forming liquids

Jennifer A. Hodgdon and Frank H. Stillinger

AT&T Bell Laboratories, Murray Hill, New Jersey 07974

The Stokes-Einstein relation $D = k_B T/(C\eta a)$ (η is the shear viscosity; D is the diffusion constant; $C = 6\pi$ for no-slip and 4π for slip boundary conditions; a is the molecular diameter) holds over a wide temperature range in many liquids. However, in a variety of fragile glass-forming liquids, a, as defined by the above expression, becomes smaller with decreasing temperature as the glass transition is approached. In an attempt to explain this experimental result, we propose that special thermal fluctuations cause domains in the liquid to become temporarily more fluidized, so that a diffusing particle can move through fluidized regions, but is inhibited from moving in the unfluidized region. We introduce a mean-field picture of this fluctuating fluid, and solve two versions for their hydrodynamic flow fields. The resulting reduced drag force can account for the violation of the Stokes-Einstein relation seen in fragile glass-forming liquids, with plausible values for the size of the fluidized region and the mean-field reduction in viscosity.

I. INTRODUCTION

The Stokes-Einstein relation gives the diffusion constant D of a particle of radius a in a fluid of shear viscosity η at temperature T:

$$D = \frac{k_B T}{C\eta a} , \qquad (1)$$

where C is a constant that ranges from 6π under no-slip boundary conditions for the fluid on the particle surface to 4π under slip boundary conditions. This relation was derived by Einstein in 1905 [1], using the Stokes formula for the drag force on a macroscopic sphere, and should, strictly speaking, only apply to diffusing particles that are much larger than the molecules comprising the fluid. However, it has been well established that it holds not only for diffusion of large particles, but also for diffusion of small tracer particles and self-diffusion in many fluids. The reason for this is still largely mysterious, but the usefulness of the Stokes-Einstein relation for predicting diffusion constants in fluids cannot be denied.

On the other hand, materials certainly exist for which the Stokes-Einstein relation fails. Two extreme examples are superfluid helium, which has a vanishing viscosity but a finite tracer diffusion constant, and elastic single crystals, which have effectively infinite viscosity but finite diffusion constants owing to the presence of mobile interstitials and vacancies. When we rewrite Eq. (1) in the following form,

$$\frac{D\eta}{T} = \frac{C'}{a} , \qquad (2)$$

and interpret a as an effective length characterizing the product of diffusion constant and viscosity, it is interesting to note that a is infinite for the superfluid, which is in a state of momentum condensation, and zero for the single crystal, which is in a state of virtually complete spatial ordering.

Many fragile glass-forming liquids also deviate from the Stokes-Einstein relation, though not in as extreme a manner as superfluids and single crystals. (The term fragile comes from a classification scheme developed in Refs. [2] and [3].) Instead, a wide variety of these materials [4–7] exhibit a length a that has the Stokes-Einstein value (i.e., the radius of the diffusing particle) at high temperatures, but that gradually decreases by as much as a factor of 3 as the temperature is lowered towards the glass transition (see Fig. 1). This behavior has also been clearly seen in recent simulations of soft-sphere [8] and Lennard-Jones [9] liquids. Furthermore, Spaepen has presented evidence that in artificial layered samples of metallic glasses [10,11], the linear relaxation rates of η and $1/D$ are inconsistent with the Stokes-Einstein relation. Other experiments on these materials [12] have shown that in the later, nonlinear stages, the relaxation curves for η and $1/D$ are quite different, again violating the Stokes-Einstein relation. However, it is not entirely clear that this is related to the violation of the Stokes-Einstein relation seen in fragile glass-formers, since these are *solid* metallic glass materials, and they are undergoing rapid relaxation.

Other transport coefficients can also be related to the viscosity in Stokes-Einstein-like relations, and these are also violated in the manner of Fig. 1 in glass-forming liquids. For example, the Stokes-Einstein-like relation between the electrical conductivity and the viscosity is violated in low-temperature glassy ionic melts and solutions [5,13,14]. There are also claims of both violation [5,15] and nonviolation [4,16] of the Debye relation between the orientational diffusion time and the viscosity in fragile glass-formers. However, when the data from, e.g., Ref. [16] is plotted in the manner of Fig. 1, we find that the Debye relation is violated in the same manner as is the Stokes-Einstein relation.

One can imagine several different explanations for low-temperature deviations from Stokes-Einstein
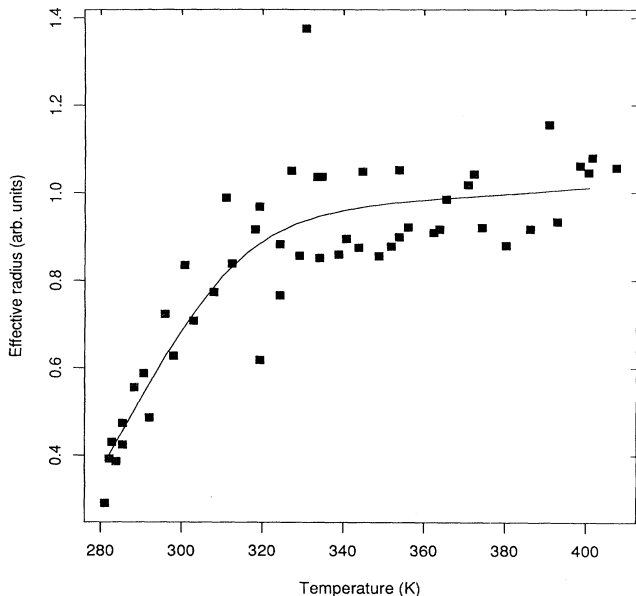
FIG. 1. Plot of experimental data from Ref. [4]: effective hydrodynamic radius [proportional to $T/(D\eta)$] in orthoterphenyl as a function of the absolute temperature. The squares are data points, and the solid line is a guide to the eye. The hydrodynamic radius is approximately constant at high temperatures, and decreases as the temperature is lowered into the supercooled region. Note that the glass-transition temperature in orthoterphenyl is approximately 243 K [4].

behavior in glass-forming liquids. For instance, cooling could cause molecules in the liquid to stick together occasionally and move in groups instead of alone—but this would *increase* the effective hydrodynamic radius a, and we know of no experiments in glass-formers where the deviation is in that direction. Another possibility is to use the result that polycrystalline solids in shear flow obey Eq. (1) with a reduced by $(V_m/V_g)^{2/3}$, where V_m and V_g are the volumes of a single molecule and a crystalline grain in the material, respectively [17]. This is appealing because a glass-forming liquid could have effective "grains" the size of individual molecules at high temperatures, and larger grains at lower temperatures; that would decrease the effective a at low temperatures in agreement with experiment. However, we cannot literally accept this scenario as the explanation for the Stokes-Einstein deviation in glass-forming liquids, because it has been well established [18] that glasses, and in particular fragile glasses, do not incorporate well-formed crystalline grains.

Instead, in this paper we propose another explanation: that the Stokes solution for the fluid velocity around a spherical diffusing particle might be modified, near the particle, by the presence of inhomogeneities arising from a special type of thermal fluctuation. These thermal fluctuations, akin to those proposed long ago by Adam and Gibbs [19], cause microscopic domains to become more fluidized, temporarily allowing enhanced diffusive flow;

outside the fluctuating regions, the liquid is more viscous, and diffusive flow is retarded. We find that this model can easily account for the typical factor-of-3 violation of the Stokes-Einstein relation seen in experiments. It also suggests the qualitative way that local flow around a diffusing particle deviates from that of the standard Stokes-Einstein description.

The simplest way to model such thermal fluctuations is to adopt a two-zone mean-field hydrodynamics, along the same vein as the model used by Zwanzig for his fluctuating diffusion problem [20]. This model, where the viscosity has one value inside the inner zone and a different value in the outer zone, has also been used by Goodstein [21] in a different context to explain ion mobility in superfluid helium. In Sec. II, we present the two-zone calculation, elaborating on the results of Goodstein, and apply it to our problem.

This two-zone model, though having some of the characteristics needed to model the special thermal fluctuations in viscosity, is somewhat unphysical. So, in Sec. III, we present a second model, where the viscosity varies smoothly in space instead of displaying a sharp boundary. We find that the hydrodynamic drag on a diffusing particle in the continuum model agrees well with the results from the simpler two-zone model, and is at least as adept at fitting the experiments. In Sec. IV, we discuss these results and their mean-field character, and suggest further experimental and theoretical work.

II. TWO-ZONE MODEL

In the Stokes solution for steady-state fluid flow around a stationary sphere of radius R, which is the origin of the denominator on the right-hand side of Eq. (1), the fluid is assumed to be incompressible, and to be flowing with low Reynolds number. This leads to two partial differential equations for the fluid velocity v_i [22]: a linearized Navier-Stokes equation,

$$\eta \frac{\partial^2 v_i}{\partial x_k^2} = \frac{\partial p}{\partial x_i} , \tag{3}$$

where p is the pressure and repeated indices indicate summation, and an equation of continuity,

$$\frac{\partial v_i}{\partial x_i} = 0 . \tag{4}$$

The boundary conditions for the fluid on the sphere can be chosen in many different ways; the two extremes are the no-slip boundary condition, where the fluid velocity vanishes on the sphere's surface, and the slip boundary condition, where the normal velocity and tangential force vanish on the surface. The other boundary condition is that, far from the sphere, the velocity of the fluid is $u\hat{z}$, unperturbed by the particle. In the no-slip case, the solution to Eq. (3) and Eq. (4) in spherical (r,θ,ϕ) coordinates, with θ measured from the z axis, is [22]

$$v_r^0 = u\,(\cos\theta)\left[1 - \frac{3R}{2r} + \frac{R^3}{2r^3}\right],$$

$$v_\theta^0 = -u\,(\sin\theta)\left[1 - \frac{3R}{4r} - \frac{R^3}{4r^3}\right]. \tag{5}$$

In the slip case, the solution is

$$v_r^0 = u\,(\cos\theta)\left[1 - \frac{R}{r}\right],$$

$$v_\theta^0 = -u\,(\sin\theta)\left[1 - \frac{R}{2r}\right]. \tag{6}$$

In both cases, the total drag force on the sphere is calculated from the integral, over the surface of the sphere, of the quantity [22]

$$-p\cos\theta + \sigma'_{rr}\cos\theta - \sigma'_{r\theta}\sin\theta$$

$$= (\cos\theta)\left[-p + 2\eta\frac{\partial v_r}{\partial r}\right]$$

$$-\eta(\sin\theta)\left[\frac{1}{r}\frac{\partial v_r}{\partial\theta} + \frac{\partial v_\theta}{\partial r} - \frac{v_\theta}{r}\right], \tag{7}$$

where σ'_{ij} is the viscous part of the stress tensor. The integral is $6\pi\eta Ru$ under no-slip boundary conditions, and $4\pi\eta Ru$ under slip conditions.

Now, instead of a homogeneous fluid, we consider a fluid with a local domain of altered viscosity. For simplicity, we assume a spherical domain of radius L, concentric with the diffusing spherical particle, as in the previous calculation by Goodstein [21]. Inside the domain, the viscosity is η^i, and outside, it is η^o (see Fig. 2). Both inside and outside, the Navier-Stokes equation (3) and equation of continuity (4) hold, with η replaced by the appropriate viscosity for the region. The boundary conditions are as in the homogeneous case, with the additional conditions that the fluid velocity and transmitted force must match at the interface between the two domains.
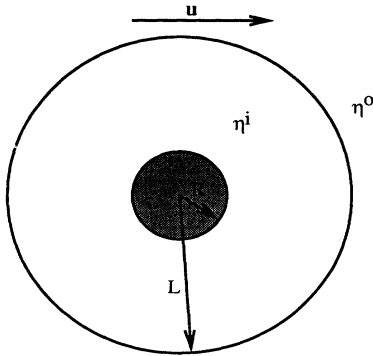

FIG. 2. Diagram of the two-zone fluid used in the hydrodynamic calculation. The spherical particle of radius R is centered in a spherical domain of radius L. Inside the domain, the fluid has viscosity η^i, and outside, it has viscosity η^o. Far from the particle, the fluid is flowing with velocity $\mathbf{u} = u\hat{\mathbf{z}}$.

Because of the symmetry of the problem, a solution to the hydrodynamic equations has the form [21]

$$v_r = u\,(\cos\theta)f(r),$$

$$v_\theta = -u\,(\sin\theta)g(r); \tag{8}$$

to satisfy Eq. (4), we must have

$$g(r) = \frac{r}{2}f'(r) + f(r). \tag{9}$$

The gradient of the pressure appearing on the right-hand side of Eq. (3) is an unknown in this problem, so Eq. (3) is satisfied whenever the curl of its left-hand side is zero. For the $\mathbf{v}$ of Eq. (8), this means that in each region,

$$\frac{4}{r^2}f'(r) - \frac{4}{r}f''(r) - 4f'''(r) - \frac{r}{2}f^{IV}(r) = 0, \tag{10}$$

for all r. The general solution to Eq. (10) is found by repeated integration; it can be written as [21]

$$f(r) = C_1\frac{r^2}{R^2} + C_2 + C_3\frac{R}{r} + C_4\frac{R^3}{r^3}, \tag{11}$$

where the C_n are dimensionless constants, determined in each region by the boundary conditions. In fact, the $r \to \infty$ boundary condition requires that in the outer region [21],

$$f^o(r) = 1 + C_5\frac{R}{r} + C_6\frac{R^3}{r^3}; \tag{12}$$

the inner solution f^i has the full form of Eq. (11).

The boundary conditions at $r = R$ and $r = L$ provide six linear equations for the six C_n, in terms of the ratios $l = L/R$ and $\zeta = \eta^o/\eta^i$; the equations, and their solutions, are shown in the Appendix. To find the drag force on the sphere, we need, in addition to the velocity, the pressure, which is obtained by integrating Eq. (3). The Laplacian of the velocity field of Eq. (8) is

$$\nabla^2\mathbf{v} = u\hat{\mathbf{r}}(\cos\theta)\left[\frac{4}{r}f'(r) + f''(r)\right]$$

$$-u\hat{\boldsymbol{\theta}}(\sin\theta)\left[\frac{2}{r}f'(r) + 3f''(r) + \frac{r}{2}f'''(r)\right], \tag{13}$$

where $\hat{\mathbf{r}}$ and $\hat{\boldsymbol{\theta}}$ are unit vectors in the radial and polar-angle directions. Equation (3) says that this is equal to the gradient of the pressure divided by the viscosity,

$$\frac{\nabla p}{\eta} = \hat{\mathbf{r}}\frac{1}{\eta}\frac{\partial p}{\partial r} + \hat{\boldsymbol{\theta}}\frac{1}{r\eta}\frac{\partial p}{\partial\theta}. \tag{14}$$

When the curl of Eq. (13) is zero, the pressure can easily be found from the $\hat{\boldsymbol{\theta}}$ component of Eq. (13) to be

$$p = \eta u\,(\cos\theta)\left[2f'(r) + 3rf''(r) + \frac{r^2}{2}f'''(r)\right]. \tag{15}$$

Given this pressure field, we can now evaluate the drag force by integrating Eq. (7) over the surface of the sphere at $r = R$, and we find that it is
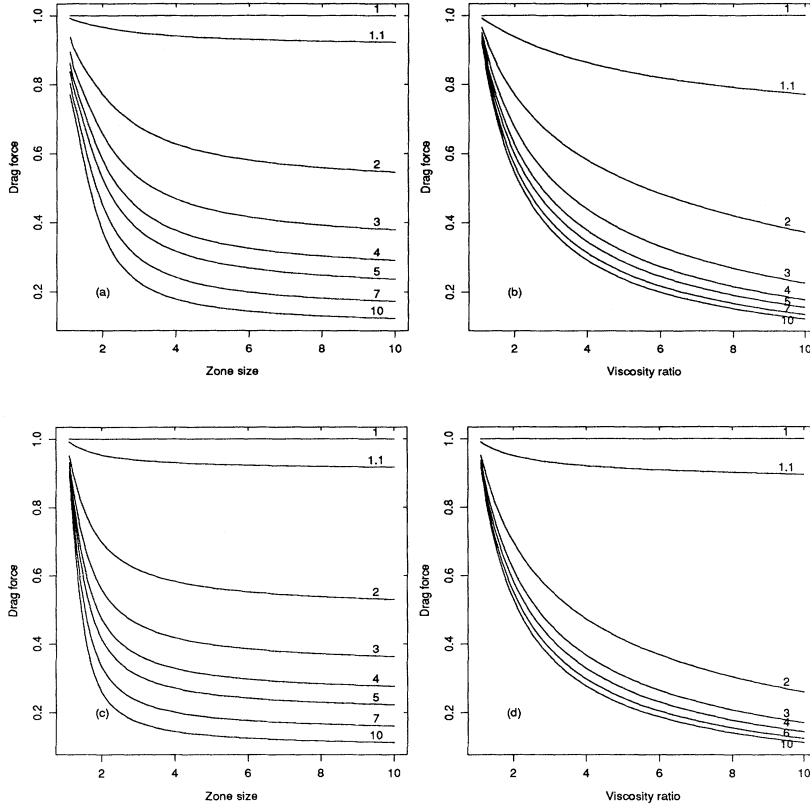
FIG. 3. Plots of the drag force in the two-zone model. (a) shows the drag force under no-slip boundary conditions, in units of $6\pi\eta^o Ru$, vs $l\equiv L/R$, for several values of $\zeta\equiv\eta^o/\eta^i$, which label the curves; (b) shows the same drag force vs ζ for several values of l. (c) and (d) are the plots for slip boundary conditions, with the drag force in units of $4\pi\eta^o Ru$. In both cases, a force of 1 means that the drag force is unchanged from the standard Stokes hydrodynamic solution; this occurs when $\zeta=1$ or $l=1$, since either condition means there is really only one zone. We only plot $\zeta>1$, since $\zeta<1$ increases the drag force.

$$F = \tfrac{2}{3}\pi\eta^i Ru\,[4Rf^{i'}(R) - 4R^2 f^{i''}(R) - R^3 f^{i'''}(R)]$$

$$= -4\pi\eta^i Ru C_3 \ . \tag{16}$$

The total force must be the same over any surface in the fluid enclosing the sphere, so we can also choose to evaluate it at $r\to\infty$; this yields

$$F = -4\pi\eta^o Ru C_5 \ , \tag{17}$$

which agrees with Goodstein's result [21]. Since $C_3=\zeta C_5$, as can be seen in Eq. (A10) and Eq. (A12), the two expressions for the drag force are equal; also, they reduce to the Stokes drag force when $\zeta=1$ or $l=1$. We exhibit plots of the drag force as a function of l and ζ in Fig. 3.

III. CONTINUUM MODEL

The two-zone model of Sec. II is somewhat satisfying, in that it provides a picture that is easy to grasp and that the calculated drag force is consistent with the experimentally observed reduction in glass-forming liquids. However, in real glass-forming liquids, we do not expect a sharp boundary between the lower-viscosity region and the bulk liquid. As a first step towards generalizing our hydrodynamic calculation to a more realistic description, we found that a three-zone model gave similar results to the two-zone model—but this still does not rule out the possibility that the presence of a sharp boundary between the zones plays a strong role in the hydrodynamic drag.

For that reason, in this section we adopt a model with a smoothly varying, spherically symmetric viscosity.

We take the viscosity to be $\eta(r)=\eta^0+\eta^1(r)$, where η^0 is the viscosity far from the particle, and $\eta^1(r)$ is a short-ranged, smooth function. When the viscosity is not piecewise constant, the linearized Navier-Stokes equation (3) becomes

$$\frac{\partial p}{\partial x_i} = \frac{\partial}{\partial x_k}\left[\eta\left[\frac{\partial v_k}{\partial x_i}+\frac{\partial v_i}{\partial x_k}\right]\right]$$

$$= \left[\frac{\partial\eta}{\partial x_k}\right]\left[\frac{\partial v_i}{\partial x_k}+\frac{\partial v_k}{\partial x_i}\right]+\eta\frac{\partial^2 v_i}{\partial x_k^2} \ , \tag{18}$$

using the incompressible-fluid equation of continuity (4) in the second expression. In addition to the equation of continuity, the $r=\infty$ boundary conditions remain the same as in the two-zone calculation, which means that we want to search for hydrodynamic solutions of the form

$$v_r = u\,(\cos\theta)\left[1-\frac{aR}{r}+\frac{bR^3}{r^3}+f(r)\right] \ ,$$

$$\tag{19}$$

$$v_\theta = -u\,(\sin\theta)\left[1-\frac{aR}{2r}-\frac{bR^3}{2r^3}+\frac{r}{2}f'(r)+f(r)\right] \ ,$$

where $f(r)$ is short ranged; the fluid flow field must also satisfy the $r=R$ slip or no-slip boundary condition. With this fluid velocity, the hydrodynamic drag force on the particle is

$$F = 4\pi\eta^0 Rua \ . \tag{20}$$

The right-hand side of Eq. (18), with the above expressions for the fluid velocity and viscosity, is

$$u\hat{r}(\cos\theta)\left\{(\eta^0+\eta^1)\left[\frac{4}{r}f'(r)+f''(r)+\frac{2aR}{r^3}\right]+\frac{\partial\eta^1}{\partial r}\left[2f'(r)+\frac{2aR}{r^2}-\frac{6bR^3}{r^4}\right]\right\}$$

$$-u\hat{\theta}(\sin\theta)\left\{(\eta^0+\eta^1)\left[\frac{2}{r}f'(r)+3f''(r)+\frac{r}{2}f'''(r)-\frac{aR}{r^3}\right]+\frac{\partial\eta^1}{\partial r}\left[f'(r)+\frac{r}{2}f''(r)+\frac{3R^3b}{r^4}\right]\right\} \ ; \tag{21}$$

as in the two-zone calculation, the curl of this quantity must be zero to satisfy Eq. (18), whose left-hand side is the gradient of the pressure. This means that

$$(\eta^0+\eta^1)\left[\frac{4}{r}f'(r)-4f''(r)-4rf'''(r)-\frac{r^2}{2}f^{\mathrm{IV}}(r)\right]$$

$$+\frac{\partial\eta^1}{\partial r}\left[-f'(r)-5rf''(r)-r^2f'''(r)\right.$$

$$\left.+\frac{3aR}{r^2}+\frac{3bR^3}{r^4}\right]$$

$$-\frac{\partial^2\eta^1}{\partial r^2}\left[rf'(r)+\frac{r^2}{2}f''(r)+\frac{3R^3b}{r^3}\right]=0 \ . \tag{22}$$

We can integrate this equation once to find that

$$\eta^0\left[2r^2f'(r)-2r^3f''(r)-\frac{r^4}{2}f'''(r)\right]$$

$$+\eta^1\left[2r^2f'(r)-2r^3f''(r)-\frac{r^4}{2}f'''(r)+3aR\right]$$

$$+\frac{\partial\eta^1}{\partial r}\left[-r^3f'(r)-\frac{r^4}{2}f''(r)-\frac{3R^3b}{r}\right]=0 \ ;$$

the integration constant must be zero if $f(r)$ is short ranged.

This equation is not integrable in closed form for arbitrary $\eta^1(r)$; however, it is straightforward to integrate it numerically to find the $f(r)$ corresponding to a given $\eta^1(r)$ and either the no-slip or slip boundary conditions at $r=R$. In fact, the two boundary conditions at $r=R$ serve to determine a and b, and therefore the drag force. We have performed this integration, taking $\eta^1=\eta^0(1/\zeta-1)\exp[(R-r)/L]$ (so that ζ is the ratio of the viscosity at $r=\infty$ to that at $r=R$), for $L=2R$ and $L=5R$ and several values of ζ. As can be seen in Fig. 4, the resulting drag force is similar to the two-zone result.

IV. DISCUSSION

We want to apply these results to glass-forming liquids that violate the Stokes-Einstein relation. In these liquids, as discussed in Sec. I, special thermal fluctuations [19] can arise that cause small regions in the extremely viscous liquid to become temporarily fluidized. In the fluidized regions, motion of a diffusing particle is much easier than in the nonfluidized region, perhaps so much that we can entirely neglect any motion of the particle through the nonfluidized region. When this is the case, we can make an effective mean-field picture of the fluid where the viscosity far from the diffusing particle has the measured macroscopic viscosity of the fluid, but near the particle, the local viscosity is reduced. The effective reduced viscosity in this picture is not as small as the viscosity of the fluctuating fluidized regions, but includes a correction for the probability of the particle to be in a fluidized region. Still, the reduction should be appreciable in some region around the particle. It is simplest to assume that the effective mean-field viscosity is spherically symmetric around the particle, and with this assump-
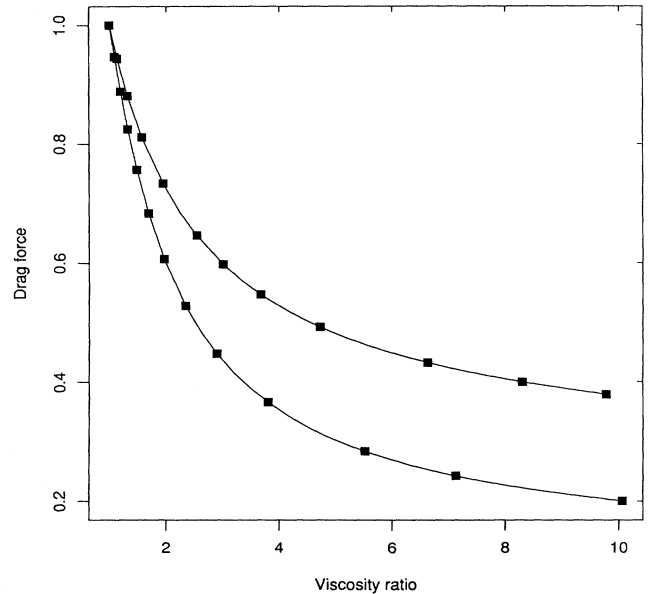

FIG. 4. Plot of the drag force when the viscosity relaxes exponentially with distance from the surface of the sphere. We show a plot of drag force, in units of $6\pi\eta^0Ru$, under no-slip boundary conditions vs the ratio of the viscosity at $r=\infty$ to the viscosity at $r=R$. The upper curve has an exponential length scale of $2R$, and the lower curve, $5R$. Squares are data points from numerical integration, and the lines are guides to the eye.

tion, the mean-field picture resembles the models considered in our hydrodynamic calculations. We expect nonspherically symmetric models to be similar, though lacking the computational simplicity of the spherically symmetric case that led us to consider it.

The experimental violation of the Stokes-Einstein relation in glass-forming liquids near the glass-transition temperature corresponds to a reduction in the drag force by about a factor of 3 from the value of the Stokes drag in a fluid with the measured viscosity of the glass-former; in our mean-field picture, the measured viscosity corresponds to the viscosity η^o or η^0 far from the particle. Our calculated hydrodynamic drag force, as seen in Fig. 3 or Fig. 4, is reduced by about a factor of 3 when, e.g., ζ, the ratio of the viscosity at $r = \infty$ to the viscosity at the particle surface, is 5, and L, the length scale for the reduced viscosity zone—either the inner-zone radius or the exponential length scale—is $5R$. In fact, for any value of L, there is some ζ for which the drag force reduction is about a factor of 3, and over some range, these values of L and ζ are plausibly obtainable from the effective mean-field picture of the thermal fluctuations.

The "jump-diffusion" behavior seen in the molecular-dynamics simulations of Barrat, Roux, and Hansen [8] appears to confirm our picture of fluctuating fluidized regions, where a diffusing particle moves only slightly unless it is in one of the fluidized regions. It would also be interesting to compare the time-averaged flow pattern around such a diffusing particle to our calculated flow pattern, to check the validity of the mean-field picture we have introduced.

Finally, we note that in our picture of the fragile glass-forming liquid, the presence of small fluctuating domains of enhanced fluidity should make the viscosity wave-vector dependent: the viscosity at short wavelengths would be reduced from that at large wavelengths. It is possible to derive Kubo relations for a wave-vector-dependent viscosity, and these could also be evaluated in simulations of glass-forming liquids, to test the validity of our picture.

ACKNOWLEDGMENT

The authors would like to express their gratitude to Dr. Robert W. Zwanzig for pointing out the existence of Ref. [21].

APPENDIX: DETAILS OF TWO-ZONE SOLUTION

In this appendix, we apply the boundary conditions to find the velocity field for a spherical particle of radius R diffusing through a locally nonuniform fluid that has viscosity η^i within a sphere of radius L centered on the particle and viscosity η^o outside of the sphere, and that is moving with velocity $u\hat{z}$ far from the diffusing particle. Incorporating the $r \to \infty$ boundary condition, we have from Sec. II the velocity field

$$v_r = u(\cos\theta)f(r) ,$$

$$v_\theta = -u(\sin\theta)\left[\frac{r}{2}f'(r) + f(r)\right] ,$$

(A1)

with

$$f(r) = \begin{cases} f^i(r) = C_1\dfrac{r^2}{R^2} + C_2 + C_3\dfrac{R}{r} + C_4\dfrac{R^3}{r^3} , \\ \qquad\qquad\qquad \text{for } R < r < L , \\ f^o(r) = 1 + C_5\dfrac{R}{r} + C_6\dfrac{R^3}{r^3}, \quad \text{for } r > L . \end{cases}$$

(A2)

The remaining boundary conditions are that at $r = R$, the radial velocity is zero, and the tangential velocity (no-slip boundary condition) or tangential force (slip boundary condition) is zero; and at $r = L$, the radial and tangential velocities match inside and outside the sphere, and the forces on the surface from the two sides are equal and opposite.

The $r = R$ boundary conditions require that

$$f^i(R) = 0 = C_1 + C_2 + C_3 + C_4 ,$$

(A3)

and that for no-slip boundary conditions,

$$f^{i'}(R) = 0 = (2C_1 - C_3 - 3C_4)/R ,$$

(A4)

while for slip boundary conditions,

$$f^{i'}(R) = -Rf^{i''}(R)/2 ,$$

or

(A5)

$$0 = 3C_1 + 3C_4 .$$

The $r = L$ boundary conditions require that

$$f^i(L) = f^o(L) ,$$

or

(A6)

$$C_1 l^2 + C_2 + C_3 l^{-1} + C_4 l^{-3} = 1 + C_5 l^{-1} + C_6 l^{-3} ,$$

where $l \equiv L/R$, that

$$f^{i'}(L) = f^{o'}(L) ,$$

or

(A7)

$$2C_1 l - C_3 l^{-2} - 3C_4 l^{-4} = -C_5 l^{-2} - 3C_6 l^{-4} ,$$

that

$$\sigma_{rr}^i(L) = \sigma_{rr}^o(L) ,$$

or

(A8)

$$6C_1 l + 3C_3 l^{-2} + 6C_4 l^{-4} = \zeta(3C_5 l^{-2} + 6C_6 l^{-4}) ,$$

where σ_{ij} is the stress tensor, and $\zeta \equiv \eta^o/\eta^i$, and finally that

$$\sigma_{r\theta}^i(L) = \sigma_{r\theta}^o(L) ,$$

or

(A9)

$$3C_1 l + 3C_4 l^{-4} = 3\zeta C_6 l^{-4} .$$

These six equations in the six unknowns C_n can be solved to find that, under no-slip boundary conditions,

$$C_1 = 3\zeta(\zeta-1)l(1-l)(1+l)/D_{NS} \ ,$$

$$C_2 = l\zeta[9-5l^2+6l^5+\zeta(-9+5l^2+4l^5)]/D_{NS} \ ,$$

$$C_3 = 3l\zeta[-2-3l^5+2\zeta(1-l^5)]/D_{NS} \ ,$$

$$C_4 = l^3\zeta[2+3l^3+2\zeta(l^3-1)]/D_{NS} \ ,$$

$$C_5 = 3l[-2-3l^5+2\zeta(1-l^5)]/D_{NS} \ ,$$

$$C_6 = l^3[2+3l^5-\zeta(2-5l^3+3l^5)]/D_{NS} \ ,$$

(A10)

where

$$D_{NS} = 4+6l^5+\zeta(-8+9l-10l^3+3l^5+6l^6)$$
$$+ \zeta^2(l-1)^4(4+7l+4l^2) \ .$$

(A11)

Under slip boundary conditions,

$$C_1 = \zeta(1-\zeta)l^3/D_S \ ,$$

$$C_2 = -\zeta l[3-3l^5-\zeta(3+2l^5)]/D_S \ ,$$

$$C_3 = \zeta l[3-3l^5-\zeta(3+2l^5)]/D_S \ ,$$

$$C_4 = \zeta(\zeta-1)l^3/D_S \ ,$$

$$C_5 = l[3-3l^5-\zeta(3+2l^5)]/D_S \ ,$$

$$C_6 = (1-\zeta)l^3(l^5-1)/D_S \ ,$$

(A12)

where

$$D_S = -2+2l^5+\zeta(4-3l+l^5+3l^6)$$
$$+ \zeta^2(l-1)^3(1+l)(2+l+2l^2) \ .$$

(A13)

[1] A. Einstein, Ann. Phys. (N.Y.) **17**, 549 (1905).

[2] C. A. Angell, in *Relaxation in Complex Systems,* Proceedings of the Workshop on Relaxation Processes, Blacksburg, VA, 1983, edited by K. Ngai and G. B. Smith (National Technical Information Service, U.S. Department of Commerce, Washington, DC, 1985), p. 3.

[3] C. A. Angell, J. Non-Cryst. Solids **73**, 1 (1985).

[4] F. Fujara, B. Geil, H. Sillescu, and G. Fleischer, Z. Phys. B **88**, 195 (1992).

[5] E. Rössler, Phys. Rev. Lett. **65**, 1595 (1990).

[6] D. Ehlich and H. Sillescu, Macromolecules **23**, 1600 (1990).

[7] N. A. Walker, D. M. Lamb, S. T. Adamy, J. Jonas, and M. P. Dare-Edwards, J. Phys. Chem. **92**, 3675 (1988).

[8] J.-L. Barrat, J.-N. Roux, and J.-P. Hansen, Chem. Phys. **149**, 197 (1990).

[9] D. Thirumalai and R. D. Mountain, Phys. Rev. E **47**, 479 (1993).

[10] F. Spaepen, Mater. Res. Soc. Symp. Proc. **37**, 295 (1985).

[11] F. Spaepen, Mater. Sci. Eng. **97**, 403 (1988).

[12] Y. Limoge and G. Brebec, Acta Metall. **36**, 665 (1988).

[13] C. T. Moynihan, N. Balitactac, L. Boone, and T. A. Litovitz, J. Chem. Phys. **55**, 3013 (1971).

[14] R. Bose, R. Weiler, and P. B. Macedo, Phys. Chem. Glasses **11**, 117 (1970).

[15] E. W. Fischer, E. Donth, and W. Steffen, Phys. Rev. Lett. **68**, 2344 (1992).

[16] C. H. Wang, R. J. Ma, G. Fytas, and Th. Dorfmüller, J. Chem. Phys. **78**, 5863 (1983).

[17] C. Herring, J. Appl. Phys. **21**, 437 (1950).

[18] R. Zallen, *The Physics of Amorphous Solids* (Wiley, New York, 1983), p. 73.

[19] G. Adam and J. H. Gibbs, J. Chem. Phys. **43**, 139 (1965).

[20] R. Zwanzig, Chem. Phys. Lett. **164**, 639 (1989).

[21] D. L. Goodstein, Phys. Rev. B **15**, 5210 (1977).

[22] L. D. Landau and E. M. Lifshitz, *Fluid Mechanics,* 2nd ed. (Pergamon, New York, 1987).